Convective instabilities of chemical fronts in close-packed porous media

Gábor Schuszter, Dezső Horváth, Ágota Tóth*

Department of Physical Chemistry and Materials Science, University of Szeged, Aradi vértanúk tere 1., Szeged, H-6720, Hungary

Abstract

Spatiotemporal pattern formation in the autocatalytic chlorite–tetrathionate reaction is studied experimentally in porous media where heterogeneities are introduced as glass beads packed in a monolayer. From initially vertical planar chemical fronts in a vertical slab, asymmetric convective structures with stable geometry evolve which propagate horizontally with constant speed. The single convection roll is characterized by its mixing length which scales with both the solution height and the permeability of the system.

Key words: reactive interface, convective instability, scaling law
PACS: 47.20.Bp, 47.54.-r, 47.70.Fw, 82.20.-w

1. Introduction

In miscible systems, hydrodynamic motion may alter interfaces developed between fluids with different densities, viscosities or—in the presence of free surfaces—surface tensions.[1] The interplay of transport processes with chemical reactions can be observed in chemical and pharmaceutical industry, environmental engineering, or even meteorology. Convection is exhibited as spatial dispersion of chemical pollutants, cooling of molten metals, transport in fuel cells,[2] magmatic flow, geostorage of various compounds,[3] or petrol removal from the earth. In the majority of these cases,[4, 5, 6, 7] the reaction matrices are various types of porous media. There is a vast literature on

*Corresponding author
Email addresses: schuszti@chem.u-szeged.hu (Gábor Schuszter), horvathd@chem.u-szeged.hu (Dezső Horváth), atoth@chem.u-szeged.hu (Ágota Tóth)

theoretical works[8, 9, 10, 11, 12, 13] where buoyancy-driven instabilities are coupled with chemistry in porous media but experiments mimicking reality are rare.

Chemical reaction fronts give a unique way to study hydrodynamic motion induced by chemical reactions,[14, 15, 16] because these thin reaction zones separate reactants from products by building up a constant density difference. The chlorite–tetrathionate (CT) reaction is one of the model reactions utilized to induce a self-sustained interface in spatially distributed systems.[17] The reaction with hydrogen ion being the autocatalyst, exhibits a rich variety of spatiotemporal patterns not only in simpler reaction-diffusion systems[17, 18, 19] but also in the presence of convection[15, 20] or migration[21, 22]. At room temperature, the density increases in the course of the reaction due to the change in composition, therefore in thin solutions the downward propagating planar fronts creating horizontal interfaces are hydrodynamically unstable and cellular structures evolve.[15] The upward propagating fronts can be either stable[15] or unstable[20] depending on the initial experimental conditions, since the reaction is highly exothermic and hence a local decrease in density may occur in thicker solution layers.

A vertical interface is, however, always unstable and soon becomes distorted as a single convection roll evolves in thin solutions. Scaling laws for the characteristics of the patterns, like mixing length or velocity, to solution height have been predicted theoretically[10, 23] and have been observed experimentally in the CT system.[24] The exponent is found to be 2 with the numerical modeling of simple cubic autocatalysis, while it is in the range of 1.2–1.3 in the experiments for the CT reactions. One possible reason for the disagreement is the difference in the length scales associated with the two systems. In the numerical calculations, the solution height is on the order of 1 mm, while in the experiments it is in the range of 1–4 cm. Recently, Bou Malham *et al.*[25] have suggested a saturation like function to characterize the dependence of normalized effective diffusion coefficient to the ratio of solution height over solution thickness when the width of the front is negligible, i.e., the eikonal approximation holds. This function predicts two as the exponent when the drag against the fluid flow imposed by the boundary is dominant, which is indeed the case for the theoretical studies of De Wit and co-workers. The lower exponent at the same time is valid for the conditions applied in the experiments. One further difference between calculations and experiments is that in the former porous media is presumed, while 2–3 mm thin homogeneous solution layers are utilized in the latter.

Several efforts have been made to design experiments in reaction matrices resembling porous media. Heterogeneity have been introduced into the walls of the reaction chamber as periodic grooves yielding periodic spatial variation in the solution thickness.[26, 27] If the wave number of the imposed heterogeneity matches that of the structure appearing initially at constant solution thickness, resonance amplification can be observed. When both parallel and perpendicular modulations are applied periodically,[28] the evolution of structure is unaffected, but continuous tip splitting is exhibited in the later stages of the pattern formation. D'Onofrio and co-workers[29] have engraved photographically the desired heterogeneity into photopolymers and have successfully suppressed convection at low porosity. Glass beads have also been used previously by Freytes *et al.* to create porous media.[30]

The aim of this experimental work is to determine scaling laws of mixing length and velocity to solution height and permeability of porous media where heterogeneities are constructed in the form of close-packed monolayers with glass beads. The results will then be compared with those of theoretical analysis and numerical modeling.

2. Experimental

Throughout our work, reagent-grade materials (Sigma, Aldrich) are used, except for $NaClO_2$ which has been recrystallized to reach at least 94 % purity.[31] Horizontally oriented, 42 cm long, 2, 3, 4, 5 mm thin and 1, 1.5, 2, 2.5, 3, 4 cm high vessels—so called Hele-Shaw cells[32]—with 8 mm thick Plexiglas walls are constructed to serve as reaction containers shown in Fig. 1. Borosilicate glass spheres of the same diameter as the width of the gap are placed piecewise manually into the assembled Hele-Shaw container, to create a mono-layer closed-packed porous media for the liquid to occupy the void. The solution—with composition of $[K_2S_4O_6]$ = 5 mM, $[NaClO_2]$ = 20 mM, [NaOH] = 2.5 mM, and [bromophenolblue] = 0.8 mM—is mixed at 3 °C temperature and injected into the cell which is pre-cooled down to 3 °C with a thermostat (Heto CBN 18-30) to eliminate thermal effects. A short (3–5 s) electrolysis at 3 V potential difference between a pair of thin (0.25 mm) Pt-wire electrodes produces small but sufficient amount of hydrogen ion at the anode to initiate a planar acidity front. The traveling front is monitored through an appropriate cutoff filter—to enhance the contrast between the reacted and the fresh solutions—by a monochrome charge-coupled device camera (Unibrain Fire-i 630) connected to the computer. The images

are digitized in 1–10 s intervals and later processed with standard imaging procedures.

Front position is determined by the point of inflection in the gray-scale values along the direction of propagation. The variation of light intensity due to the individual beads is diminished by applying a one-dimensional low-pass Fourier filter on the front profile. The mixing length (L_m) is then defined as the standard deviation of the front position in the direction of propagation. It is evaluated only for profiles with stable geometry and traveling at a constant velocity, i.e., after the initial transition period.

In order to quantitatively characterize our porous medium, its porosity (ϵ), defined as the ratio of the void (or free) volume to the total volume, is measured in a separate set of experiments where the reactant solution is substituted by water. The corresponding permeability (K) is determined by measuring the volume flow rate (w) of water at an applied pressure difference (Δp) across the porous medium with height (h) and cross section (A) from

$$K = \frac{w\, h\, \eta}{A\, \Delta p} \tag{1}$$

in accordance with the application of Darcy's law for steady state conditions, where η is the dynamic viscosity of water and $A = L_z L_y$ with $L_z = 4$ cm and L_y is varied according to the bead size.

3. Results & Discussion

In the chlorite–tetrathionate reaction system, the product solution is denser than the reactant one[15] under isothermal conditions. Although the reaction is highly exothermic, experiments carried out around the maximum density of the aqueous solution are free of thermal effects. Hence for a horizontally propagating vertical chemical front, the products will sink under the reactants.[33] After a transition period, an asymmetric structure develops shown in Fig. 2(a) which travels with constant velocity and has a constant shape. The chemical front propagating through our close-packed porous medium also produces a constant shape (see Fig. 2(b)) although its velocity is less than that observed in the corresponding thin homogeneous layer. The shape of the structure is similar in both cases: A single convection roll builds up and rotates counterclockwise for a reaction front traveling form left to right but the amplitude and hence, the mixing length drastically decreases in the heterogeneous set-up.

The increase of the solution height yields stronger convection even in porous medium which leads to fronts with greater mixing lengths, thus the parameters of the pattern change on increasing the height of the container. Self-similar properties are anticipated for a porous medium by previous theoretical works. Namely, the mixing length characterizing the geometry of the pattern may be scaled according to

$$L_m = A\, L_z^B. \tag{2}$$

to the height of the liquid slab with A being a constant for constant permeability. We therefore used the same relation to validate its experimental existence for the system where glass beads with a given diameter fill the entire container forming a monolayer. A reaction front with a constant shape evolves in all situations as illustrated in Figure 3, and at the same time for systems of larger beads the amplitude and hence the mixing length associated with the single convection roll increase. At this point it is important to emphasize that by increasing the diameter of the beads together with gap width of the cell, the porosity of the system does not vary significantly as summarized in Table 1. The variation is only a result of the imperfection of the packing and the fluctuation in bead size and gap width. It is indeed the permeability that increases with the bead size for the monolayer: it changes a magnitude upon increasing the bead diameter from 2 mm to 5 mm. For close packed spheres the permeability is predicted by the Carman-Kozeny model as

$$K_{CK} = \frac{\varepsilon^3\, d^2}{180(1-\varepsilon)^2} \tag{3}$$

where ε is the porosity and d is the diameter of the spheres. Except for bead diameter of 2 mm, our measured values return the proportionality with $\varepsilon^3 d^2/(1-\varepsilon)^2$, only the numerical constant of 180 should be replaced with 490 ± 10. The smaller permeability results from the fact that we have a monolayer of spheres in our porous medium. The discrepant value for porosity of the medium with the smallest beads is due to the small gap remaining between the beads and the wall, i.e., the packing was not as efficient and tight as in the rest.

Figure 4 illustrates the power law fitted to the determined mixing length according to Eqn. (2) for each bead size. The proportionality coefficients of the experimentally determined scaling laws (see Table 2) increase on increasing bead size and hence the permeability of the system. The exponent,

however, is constant within the experimental error, except for the case with beads of 2 mm in diameter, which has an exponent slightly below the rest. This tendency is the same as that observed in the homogeneous system on increasing the gap width.[33, 34] In that case the exponent is increasing in a small extent from 1.19±0.04 (of the 1 mm thin solution layer) to 1.34±0.09 (of 2 mm) and 1.31±0.08 (of 3 mm), suggesting that the exponent associated with the 1 mm thin solution layer is slightly below the rest for which it can be considered constant within the experimental error. By taking into account the porosity, our heterogeneous system yields similar results: the solution around beads 2 mm in diameter constitutes a liquid layer with an average thickness of 1 mm, while the rest would correspond to solution layers with thickness ranging from 1.5 mm to 2.5 mm. In this respect for all cases the exponents obtained in the porous media are slightly (~ 0.08) less than in the appropriate homogeneous liquid slab. The proportionality coefficients, however, are significantly different, since for porous media they are smaller by at least a factor of two compared to the corresponding homogeneous case. This is also reflected in the large difference of the mixing length shown in Fig. 2, and results from the increased drag exerted on the solution around the beads, since the area of solid-liquid interface is significantly greater in the porous medium.

In order to quantify the variation of the proportionality coefficient, the change in the mixing length is compared to the increase in permeability for a given container height, as shown in Fig. 5. The identical trend allows for a power function with a unique exponent for the permeability as well. Hence we can construct the single equation

$$L_m/\mathrm{cm} = (0.20 \pm 0.01)(L_z/\mathrm{cm})^{1.20\pm0.02}\,(K/10^{-5}\mathrm{cm}^2)^{0.32\pm0.01} \qquad (4)$$

for all parameters of our porous media.

According to Salin and co-workers[25, 35], the velocity of front propagation v should scale with the solution height approximately as $L_z^{0.12\pm0.06}$ for a stable convection roll in the chlorite–tetrathionate reaction when L_z is in the centimeter range. To address this issue, we also present the measured front velocity in this fashion in Fig. 6, while the results of the fittings are explicitly stated in Table 2. The proportionality coefficients increase with permeability similarly to that observed for the mixing length. The exponents are equal to the corresponding value for the mixing length minus one, i.e., $D = B - 1$ in Table 2—a feature proposed by Salin and measured for our reaction in homogeneous systems—, except for beads with the largest diameter.

Finally we can conclude that we have determined the scaling laws for the horizontal propagation of vertical reactive interfaces in porous media. We have shown that for approximately constant porosity on increasing the permeability of the system, both the mixing length and the velocity of propagation increases. The comparison of the characteristics of the spatiotemporal patterns for the close-packed porous media and the homogeneous solution layer reveals similar exponents in the power law associated with the single convection roll arising at the reactive interface. This existing quantitative similarity ensures the applicability of calculations based on equations describing porous media and allows experiments to characterize the phenomena in thin homogeneous solution layers.

Acknowledgment

This work was financially supported by the Hungarian Scientific Research Fund (OTKA K72365) and the European Space Agency (ESTEC 4000102255/11/NL/KML).

References

[1] I.R. Epstein, J.A. Pojman, An Introduction to Nonlinear Dynamics: Oscillations, Waves, Patterns, and Chaos, Oxford University Press, Oxford, 1998.

[2] A. Bertei, A.S. Thorel, W.G. Bessler, C. Nicolella, Chem. Eng. Sci. 68 (2012) 606.

[3] T-Y. Liu, A.N. Campbell, A.N. Hayhurst, S.S.S. Cardoso, Comb. Flame, 157 (2010) 230.

[4] J.T.H. Andres, S.S.S. Cardoso, Phys. Rev. E 83 (2011) 046312.

[5] J. Yang, A. D'Onofrio, S. Kalliadasis and A. De Wit, J. Chem. Phys. 117 (2002) 9395.

[6] J. Martin, N. Rakotomalala, D. Salin, Phys. Rev. E 65 (2002) 051605.

[7] C. Almarcha, P.M.J. Trevelyan, P. Grosfils, A. De Wit, Phys. Rev. Lett. 104 (2010) 044501.

[8] A. De Wit, Phys. Rev. Lett. 87 (2001) 054502.

[9] D.I. Coroian, D.A. Vasquez, J. Chem. Phys. 119, (2003) 3354.

[10] A. De Wit, Phys. Fluids 16 (2004) 163.

[11] S. Kalliadasis, J. Yang, A. De Wit, Phys. Fluids 16 (2004) 1395.

[12] L. Rongy, N. Goyal, E. Meiburg, A. De Wit, J. Chem. Phys. 127 (2007) 144710.

[13] P.M.J. Trevelyan, C. Almarcha, A. De Wit, J. Fluid. Mech. 670 (2011) 38.

[14] M. Böckmann and S. C. Müller, Phys. Rev. Lett. 85 (2000) 2506.

[15] D. Horváth, T. Bánsági, Jr., Á. Tóth, J. Chem. Phys. 117 (2002) 4399.

[16] L. Sebestiková, J.D. D'Hernoncourt, M.J.B. Hauser, S.C. Müller and A. De Wit, Phys. Rev. E 75 (2007) 026309.

[17] L. Szirovicza, I. Nagypál, E. Boga, J. Am. Chem. Soc. 111 (1990) 2842.

[18] D. Horváth, Á. Tóth, J. Chem. Phys. 108 (1998) 1447.

[19] M. Fuentes, M.N. Kuperman, P. De Kepper, J. Phys. Chem. A 105 (2001) 6769.

[20] T. Bánsági, Jr., D. Horváth, Á. Tóth, Chem. Phys. Lett. 384 (2004) 153.

[21] Z. Virányi, A. Szommer, Á. Tóth, D. Horváth, Phys. Chem. Chem. Phys. 6 (2004) 3396.

[22] Z. Virányi, Á. Tóth, D. Horváth, Chem. Phys. Lett. 401 (2005) 575.

[23] D. Lima, A. D'Onofrio, A. De Wit, J. Chem. Phys. 124 (2006) 014509.

[24] T. Tóth, D. Horváth and Á. Tóth, J. Chem. Phys. 128 (2008) 144509.

[25] I. Bou Malham, N. Jarrige, J. Martin, N. Rakotomalala, L. Talon, D. Salin, J. Chem. Phys. 133 (2010) 244505.

[26] D. Horváth, T. Tóth, Á. Tóth, Phys. Rev. Lett. 97 (2006) 194501.

[27] T. Tóth, D. Horváth, Á. Tóth, J. Chem. Phys. 127 (2007) 234506.

[28] T. Tóth, D. Horváth, Á. Tóth, Chem. Phys. Lett. 477 (2009) 315.

[29] L. Macias, D. Müller, A. D'Onofrio, Phys. Rev. Lett. 102 (2009) 094501.

[30] V.M. Freytes, A. D'Onofrio, M. Rosen, C. Allain, J.P. Hulin, Physica A 290 (2001) 286.

[31] Á. Tóth, D. Horváth and A. Siska, J. Chem. Soc., Faraday Trans. 93 (1997) 73.

[32] H.S. Hele-Shaw, Nature 58 (1898) 34.

[33] G. Schuszter, T. Tóth, D. Horváth, Á. Tóth, Phys. Rev. E 79 (2009) 016216.

[34] L. Rongy, G. Schuszter, Z. Sinkó, T. Tóth, D. Horváth, Á. Tóth, A. De Wit, Chaos 19 (2009) 023110.

[35] N. Jarrige, I. Bou Malham, J. Martin, N. Rakotomalala, D. Salin, L. Talon, Phys. Rev. E 81 (2010) 066311.

Table 1: Porosity (ε) and permeability (K) of close-packed monolayers constructed from glass beads of various diameters(d)

d (mm)	ε	$K(10^{-9}$ m$^2)$
2	0.514 ± 0.001	1.72 ± 0.01
3	0.430 ± 0.009	4.53 ± 0.04
4	0.448 ± 0.001	9.34 ± 0.03
5	0.447 ± 0.004	14.82 ± 0.51

Table 2: Proportionality coefficients and exponents in the power-law fitting of the mixing length ($L_m = A\,L_z^B$) and the front velocity ($v = C\,L_z^D$) for various glass bead diameters:

d (mm)	A	B	C	D
2	0.265 ± 0.018	1.12 ± 0.06	0.448 ± 0.007	0.124 ± 0.016
3	0.314 ± 0.005	1.22 ± 0.01	0.536 ± 0.018	0.202 ± 0.035
4	0.422 ± 0.016	1.18 ± 0.03	0.680 ± 0.010	0.203 ± 0.016
5	0.464 ± 0.009	1.22 ± 0.02	0.852 ± 0.034	0.355 ± 0.049

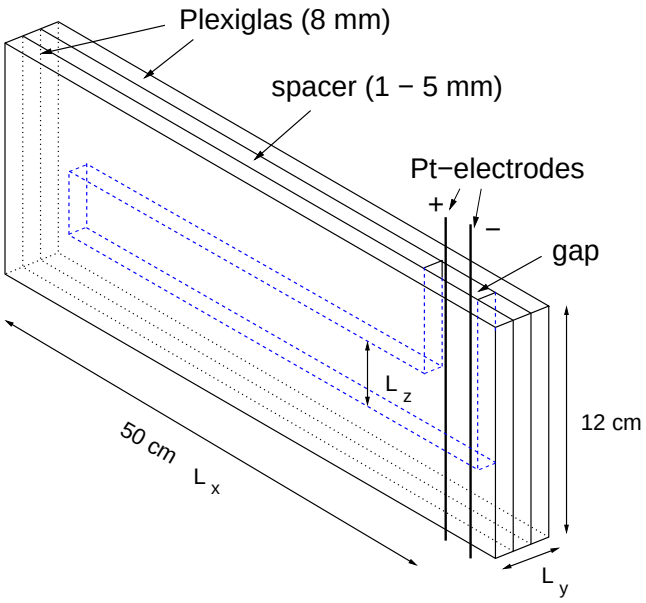

Figure 1: Scheme of the Hele-Shaw cell.

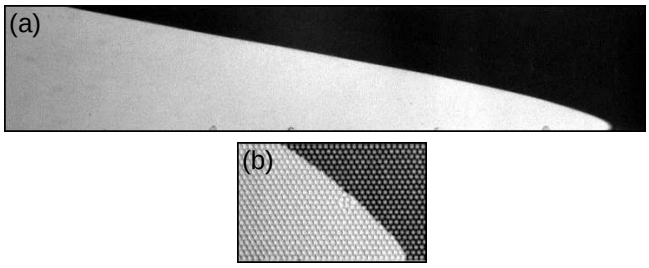

Figure 2: Images of a front in a homogeneous system (a) and in a porous medium (b) at 3 °C with a gap width of 2 mm and a liquid height of 4 cm. Field of view: 20 cm × 4 cm (a), 6 cm × 4 cm (b). Lighter region represents the denser product solution and darker one the reactant.

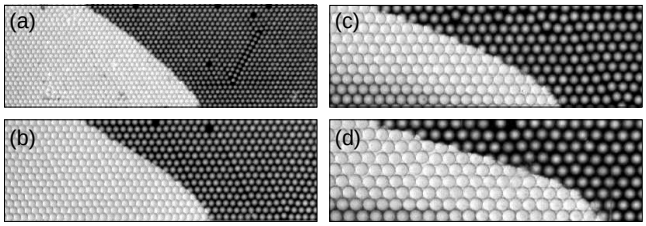

Figure 3: Images of fronts in porous media at 3 °C with bead diameter of 2 mm (a), 3 mm (b), 4 mm (c), and 5 mm (d). Field of view: 4.0 cm × 14.3 cm.

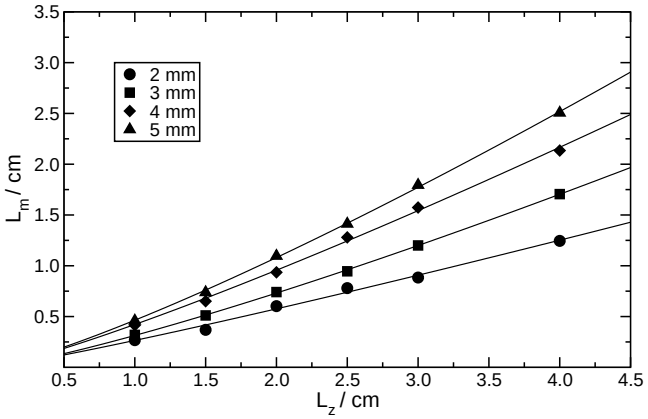

Figure 4: The mixing length (L_m) as a function of the height of the container (L_z) for various widths: 2 mm (•), 3 mm (■), 4 mm (⧫), and 5 mm (▲). The experimental errors are smaller than the size of symbols.

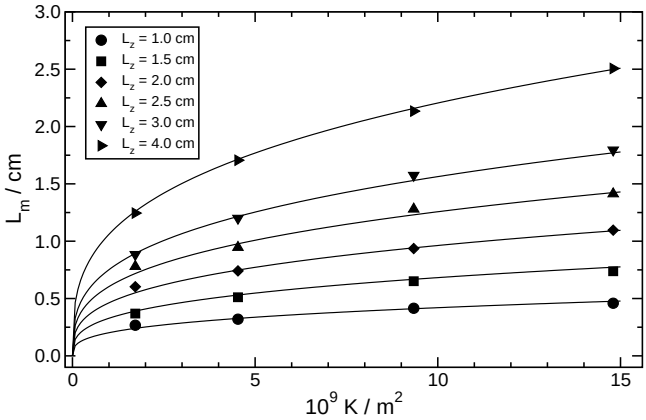

Figure 5: The mixing length (L_m) as a function of the permeability (K) for various container heights. The experimental errors are smaller than the size of symbols.

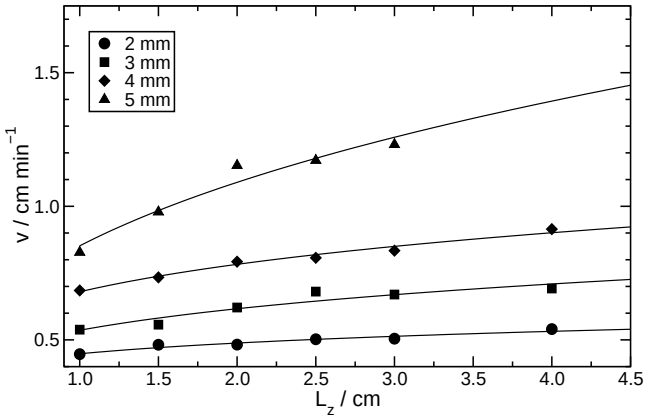

Figure 6: The front velocity (v) as a function of the height of the container (L_z) for various widths: 2 mm (●), 3 mm (■), 4 mm (⧫), and 5 mm (▲). The experimental errors are smaller than the size of symbols.